Applied Mathematics & Information Sciences
An International Journal

http://dx.doi.org/10.18576/amis/190213

Three-dimensional Boundary Element Modeling for The Effect of Rotation on the Thermal Stresses of Anisotropic Materials

Mohamed A. Fahmy[1,2,*]

[1]Department of Mathematics, Adham University College, Umm Al-Qura University, Adham, Makkah 28653, Saudi Arabia
[2]Faculty of Computers and Informatics, Suez Canal University, New Campus, Ismailia 41522, Egypt

Received: 1 Aug. 2024, Revised: 1 Sep. 2024, Accepted: 1 Oct. 2024.
Published online: 1 Mar. 2025

Abstract: The suggested 3D boundary element method (BEM) tackles the rotation effect on thermal stresses of anisotropic materials by employing the exact transformation technique, which entails analytically translating the extra domain integral to the boundary without using internal treatments. To account for thermoelastic effects in anisotropic materials, the BEM analysis was implemented by re-expressing the fundamental solutions and their derivatives as double-Fourier-series. This analytical transformation approach has completely restored the BEM's distinctive notion that just the boundary must be discretized. The revised 3D boundary integral equation (BIE) is implemented and utilized to analyze such issues. Furthermore, the studies have shown that the BEM technique is highly effective in producing accurate results for thermal stress problems in anisotropic materials.

Keywords: Three-dimensional, Boundary element method, Fundamental solutions, rotation; Thermal stresses; Anisotropic materials.

1. Introduction

Thermal stresses develop in the body due to non-uniform temperature distribution. Under a non-uniform temperature distribution, the body attempts to distort until the temperature distribution is uniform throughout the body. The distortion of the body causes forces known as thermal stresses. Thermal strains are typically avoided in the construction of building structures. However, in some constructions, thermal stresses must be induced to improve building performance. Thermal stresses are categorized as: 1) Homogeneous thermal stresses - When a body's temperature distribution is independent of time, the body can reach an equilibrium condition, resulting in homogeneous thermal strains. This sort of thermal stress appears in a variety of fields. 2) Non-homogeneous thermal stresses - When the temperature distribution in a body varies with time, the body cannot achieve equilibrium, and the resulting thermal strains are referred to as non-homogeneous thermal stresses. This sort of thermal stress occurs in numerous fields [1-4].

Thermal stresses in homogeneous isotropic solids were discovered around 1820 and have been studied since 1830, when study on the resistance of metal bars to unfired steam pipes began. Many treatises contain analytical and experimental evidence. Thermal stresses and related issues can arise in a variety of common circumstances, including solids' resistance to high temperatures, building structures, the mechanical behavior of machine parts, and civil engineering. The study of thermal stresses is interesting for both theoretical and practical reasons: it provides a basic example of a mechanical problem and demonstrates how stresses vary with temperature. Restrictions imposed on a solid body are known to cause thermal stresses that effectively limit the solid's motion. A remarkable number of recent investigations provide conclusions on this and other relevant topics, such as the performance and reliability of thermal barrier coatings against high-temperature fatigue and corrosion. [5-8].

Thermal stresses in anisotropic bodies refer to strains caused by asymmetric temperature changes in distinct places. Initially, theoretical calculations were performed to solve distinct temperature and stress-strain concerns. At the body's boundary, the normal components of the stress tensor are entirely thermal in nature. It also revealed the stress nature of thermal stresses, which are completely independent of elastic material properties when determined by solving the thermal problem or applying Fourier's theorem if the temperature at the unknown points inside the body differs from the previously obtained temperature. Thermal stresses in an isotropic elastic body are hydrostatic when computing the temperature field inside the body, and the temperature factor somewhat affects the resulting stress phase for the body; nonetheless, this has no effect on their real levels and distribution in an isotropic body. [9-11].

Anisotropic thermal expansion is a common companion of anisotropy in elastic characteristics. Most substances are polyatomic, or made of many phases, and their properties vary along different axes and orientations. These features are often characterized using directionally dependent moduli and thermal expansion coefficients. In addition to being an example of anisotropy, applying temperature or thermal gradients to anisotropic substances causes thermal stress. Many researchers have calculated and visualized

*Corresponding author e-mail: maselim@uqu.edu.sa

how these thermal stresses arise, particularly in materials having anisotropic coefficient tensors. However, most of this research has previously been qualitative in character. Many of the quantitative evaluations were limited to uniaxial instances or highly constrained geometries. A few studies have investigated the behavior using only one or two of the many parameters that describe the problem. Furthermore, the few calculations for more generic instances were all presented as severely discontinuous and difficult-to-visualize maps [12-14]. The classical linear theory of thermoelasticity states that the equilibrium equations of motion are uncoupled, and the function of thermal expansion is modified solely by temperature changes in a body. However, this property of linear theory fails when the thermal deformation of the body is considerable. As a result, the linear theory is only applicable to a narrow temperature range. However, in many engineering issues, considerable and non-uniform temperature variations might be predicted due to the presence of heating sources, external temperature gradients, or other factors in diverse machine components. These heat loads create deformities and internal tensions in the organism. The formulation of thermal stresses is difficult, first for determining the stresses caused by temperature gradients across the body, and second for the possibility of substantial deformations [15-17].

The boundary element method (BEM), also known as the method of boundary integral equations (BIE), is a modern numerical technique for solving field problems governed by a second-order partial differential equation, such as Laplace's or Helmholtz's equations for electromagnetic, heat conduction, and acoustic fields, and the elastic or linearized dynamic equation for stress or elastic wave propagation fields. That is, BEM can accomplish some jobs that are currently carried out using finite element, finite difference, method of moments, and boundary grid generation techniques [18, 19]. The fundamental advantage of BEM is that all dependent variables of importance, such as potential, stress, velocity, and displacement, are expressed in terms of integral equations of the same order as the problem's dimensions. This means that potential problems in two dimensions produce first-kind integral equations, but stress/displacement problems in three dimensions produce second-kind and hyper-singular integral equations, respectively. This key characteristic of BEM allows for a significant reduction in the number of elements or grid points necessary to achieve pre-specified accuracy, resulting in high-order polynomial accuracy and orders of magnitude reductions in memory and computational time [20-22].

To describe BEM theory, essential notions from the theory of a boundary value problem regulated by a linear, second-order partial differential equation are presented. Following that, the most critical phases in developing the BEM theory for a specific boundary value problem are discussed. Starting with the governing partial differential equation subject to the homogeneous boundary condition, the issue can be solved explicitly if the right-hand side of the equation, or source term, is already known. If the source term is unknown, the problem is simplified to a boundary integral equation [23, 24]. In the case of an unbounded domain, the Green's function of the infinite problem serves as the kernel of the integral. This means that Green's function solves the problem at all field locations of interest because of its pointwise product with the unknown source term. BIE's well-posedness property allows the solution to the original homogeneous initial-boundary value problem to be easily discovered if it is evaluated and solved immediately on the boundary [25-27].

In this paper, we develop a 3D BEM model to deal with thermoelastic phenomena and examine the influence of rotation on thermal stresses of anisotropic materials. The proposed 3D BEM used a technique that re-expressed the fundamental solutions into the forms of double Fourier series.

2 Formulation of the problem

The governing equations for thermal stresses in anisotropic materials are:

$$\frac{\partial \sigma_{ij}}{\partial x_{\mathrm{j}}} + F_i = 0, \tag{1}$$

$$\mathbb{K}_{11}\frac{\partial^2 T}{\partial x_1^2} + \mathbb{K}_{22}\frac{\partial^2 T}{\partial x_2^2} + \mathbb{K}_{33}\frac{\partial^2 T}{\partial x_3^2} + 2\mathbb{K}_{12}\frac{\partial^2 T}{\partial x_1\,\partial x_2}$$

$$+2\mathbb{K}_{13}\frac{\partial^2 T}{\partial x_1\,\partial x_3} + 2\mathbb{K}_{23}\frac{\partial^2 T}{\partial x_2\,\partial x_3} = 0 \tag{2}$$

where

$$\sigma_{ij} = C_{ijkl}(\varepsilon_{kl} - \alpha_{kl}\Delta T)\,, \quad (i,j,k,l = 1,2,3) \tag{3}$$

$$F_i = \rho\omega^2 \mathbf{x}_i - \rho \tag{4}$$

Based on the following coordinate transformation [28]

$$\mathbf{x}'^{\mathrm{T}} = \mathbb{F}\mathbf{x}^{\mathrm{T}} \tag{5}$$

with the transformation matrix

$$\mathbb{F} = \begin{pmatrix} \sqrt{\Delta}/\mathbb{K}_{11} & 0 & 0 \\ -\mathbb{K}_{12}/\mathbb{K}_{11} & 1 & 0 \\ B_1 & B_2 & B_3 \end{pmatrix} \tag{6}$$

in which

$$\forall = \mathbb{K}_{11}\mathbb{K}_{22} - \mathbb{K}_{12}^2 \tag{7}$$

$$B_1 = \frac{(\mathbb{K}_{12}\mathbb{K}_{23} - \mathbb{K}_{13}\mathbb{K}_{22})}{\sqrt{\Omega}} \tag{8}$$

$$B_2 = \frac{(\mathbb{K}_{12}\mathbb{K}_{13} - \mathbb{K}_{23}\mathbb{K}_{11})}{\sqrt{\Omega}} \tag{9}$$

$$B_3 = \frac{\forall}{\sqrt{\Omega}} \tag{10}$$

$$\Omega = \mathbb{K}_{11}\mathbb{K}_{13}\forall - \mathbb{K}_{11}\mathbb{K}_{12}\mathbb{K}_{13}^2 + \mathbb{K}_{11}\mathbb{K}_{12}\mathbb{K}_{13}\mathbb{K}_{23} - \mathbb{K}_{23}^2\mathbb{K}_{11}^2 \tag{11}$$

The heat conduction equation (2) in the transformed

coordinate system can be expressed as

$$T_{,i'i'} = 0 \tag{12}$$

3 BEM implementation for anisotropic thermoelasticity

The boundary integral equation for the considered problem is:

$$C_{ij}(\mathbb{P})\mathbb{u}_i(\mathbb{P}) + \int_C \mathbb{u}_i(\mathbb{Q})\mathbb{T}^*_{ij}(\mathbb{P},\mathbb{Q})dC = \int_C \mathbb{t}_i(\mathbb{Q})\mathbb{U}^*_{ij}(\mathbb{P},\mathbb{Q})dC + \int_R F_i(\mathbb{q})\mathbb{U}^*_{ij}(\mathbb{P},\mathbb{q})d\mathrm{R} \tag{13}$$

In the governing equations thermal, rotation and inertia impacts are treated as body forces. Thus, Eq. (13) can be written as [2]:

$$C_{ij}(\mathbb{P})\mathbb{u}_i(\mathbb{P}) + \int_C \mathbb{u}_i(Q)\mathbb{T}^*_{ij}(\mathbb{P},Q)dS = \int_C \mathbb{t}_i(\mathbb{Q})\mathbb{U}^*_{ij}(\mathbb{P},\mathbb{Q})dS + \int_C \vartheta_{ik}n_k(\mathbb{Q})T(\mathbb{Q})\mathbb{U}^*_{ij}(\mathbb{P},\mathbb{Q})dS - \int_{\mathrm{R}} \vartheta_{ik}T_{,k}(\mathbb{q})\mathbb{U}^*_{ij}(\mathbb{P},\mathbb{q})d\Omega \tag{14}$$

where

$$\vartheta_{ik} = C_{ijkl}\alpha_{jl} \tag{15}$$

Based on Ting and Lee [25], the displacement fundamental solution is

$$\mathbb{U}^*(\mathbf{x}) = \frac{1}{4\pi r}\frac{1}{|\boldsymbol{\kappa}|}\sum_{\mathrm{n}=0}^{4} q_n\Gamma^{(\mathrm{n})} \tag{16}$$

where

$$q_n = \frac{-1}{2B_1B_2B_3}\left[\mathrm{Re}\left\{\sum_{t=1}^{3}\frac{p_t^n}{(p_t - p'_{t+1})(p_t - p'_{t+2})}\right\} - \delta_{n2}\right] \text{ for } n = 0,1,2 \tag{17}$$

$$q_n = \frac{1}{2B_1B_2B_3}\mathrm{Re}\left\{\sum_{t=1}^{3}\frac{p_t^{n-2}p'_{t+1}p'_{t+2}}{(p_t - p'_{t+1})(p_t - p'_{t+2})}\right\} \text{ for } n = 3,4. \tag{18}$$

$$\Gamma^{(\mathrm{n})}_{\mathrm{ij}} = \Gamma^{(\mathrm{n})}_{(i+1)(j+1)(i+2)(j+2)} - \Gamma^{(\mathrm{n})}_{(i+1)(j+2)(i+2)(j+1)},\ (i,j = 1,2,3) \tag{19}$$

$$\kappa_{ik} = C_{ijks}\mathrm{A}_j\mathrm{A}_s \tag{20}$$

$$\mathbf{A} = (-\sin\theta', \cos\theta', 0) \tag{21}$$

$$\theta' = \tan^{-1}\left(\frac{\boldsymbol{x}_2}{\boldsymbol{x}_1}\right), \qquad \theta' \in [0,2\pi] \tag{22}$$

The Stroh's eigenvalues are

$$p_h = a_h + \mathrm{i}B_h, B_h > 0, (h = 1,2,3) \tag{23}$$

In Eq. (19), the 4th-order tensor $\boldsymbol{\Gamma}^{(n)}$ is given by

$$\Gamma^{(4)}_{\mathbb{cdef}} = \mathcal{B}_{\mathbb{cd}}\mathcal{B}_{\mathbb{ef}}, \tag{24}$$

$$\Gamma^{(3)}_{\mathbb{cdef}} = \mathcal{F}_{\mathbb{cd}}\mathcal{B}_{\mathbb{ef}} + \mathcal{B}_{\mathbb{cd}}\mathcal{F}_{\mathbb{ef}}, \tag{25}$$

$$\Gamma^{(2)}_{\mathbb{cdef}} = \mathcal{B}_{\mathbb{cd}}\mathcal{M}_{\mathbb{ef}} + \mathcal{B}_{\mathbb{ef}}\mathcal{M}_{\mathbb{cd}} + \mathcal{F}_{\mathbb{cd}}\mathcal{F}_{\mathbb{ef}}, \tag{26}$$

$$\Gamma^{(1)}_{\mathbb{cdef}} = \mathcal{F}_{\mathbb{cd}}\mathcal{M}_{\mathbb{ef}} + \mathcal{F}_{\mathbb{ef}}\mathcal{M}_{\mathbb{cd}}, \tag{27}$$

$$\Gamma^{(0)}_{\mathbb{cdef}} = \mathcal{M}_{\mathbb{cd}}\mathcal{M}_{\mathbb{ef}}. \tag{28}$$

where

$$\mathcal{B}_{ik} = C_{ijks}\mathrm{A}_j\mathrm{A}_s, \tag{29}$$

$$\mathcal{F}_{ik} = \left(C_{ijks}\mathrm{B}_j\mathrm{A}_s\right) + \left(C_{ijks}\mathrm{B}_j\mathrm{A}_s\right)^T, \tag{30}$$

$$\mathcal{M}_{ik} = C_{ijks}\mathrm{B}_j\mathrm{B}_s\,. \tag{31}$$

In Eqs. (30) and (31), B is defined by

$$\mathrm{B} = (\cos\phi'\cos\theta', \cos\phi'\sin\theta', -\sin\phi') \tag{32}$$

where

$$\phi' = \cos^{-1}(x_3/r'), \quad \left[-\frac{\pi}{2} \le \phi' \le \frac{\pi}{2}\right] \tag{33}$$

Green's function in spherical coordinates is

$$\mathbb{U}^*(r',\theta',\phi') = \frac{\mathrm{G}(\theta',\phi')}{4\pi r'} \tag{34}$$

which can be reexpressed as follows [3]:

$$\mathrm{G}_{gh}(\theta',\phi') = \sum_{\mathrm{A}=-a}^{a}\sum_{\mathrm{B}=-a}^{a}\lambda^{(\mathrm{A,B})}_{gh}\mathrm{e}^{\mathrm{i}(\mathrm{A}\theta\prime+\mathrm{B}\phi\prime)},\ (g,h = 1,2,3) \tag{35}$$

where

$$\lambda^{(\mathrm{A,B})}_{gh} = \frac{1}{4\pi^2}\int_{-\pi}^{\pi}\int_{-\pi}^{\pi}\mathrm{H}_{gh}(\theta',\phi')\mathrm{e}^{-\mathrm{i}(\mathrm{A}\theta\prime+\mathrm{B}\phi\prime)}\mathrm{d}\theta'\mathrm{d}\phi' \tag{36}$$

The first order derivatives of (34) are

$$\mathbb{U}^*_{gh,m} = \frac{\partial\mathbb{U}^*_{gh}}{\partial r'}\frac{\partial r'}{\partial \mathrm{x_l}} + \frac{\partial\mathbb{U}^*_{gh}}{\partial\theta'}\frac{\partial\theta'}{\partial \mathrm{x_l}} + \frac{\partial\mathbb{U}^*_{gh}}{\partial\phi'}\frac{\partial\phi'}{\partial \mathrm{x_l}} \tag{37}$$

Therefore, from (32) and (33), we obtain the following forms [28]:

$$\mathbb{U}^*_{gh,m} = \frac{1}{4\pi r'^2}\sum_{\mathrm{A}=-a}^{a}\sum_{\mathrm{B}=-a}^{a}\lambda^{(\mathrm{A,B})}_{gh}\mathrm{e}^{\mathrm{i}(\mathrm{A}\theta'+\mathrm{B}\phi')}\left[\frac{-\cos\theta'(\sin\phi' - \mathrm{i\,B}\cos\phi') - \mathrm{i\,A}\sin\theta'}{\sin\phi'}\right] \text{ for } m = 1, \tag{38}$$

$$\mathbb{U}^*_{gh,m} = \frac{1}{4\pi r'^2}\sum_{A=-a}^{a}\sum_{B=-a}^{a}\lambda^{(A,B)}_{gh}e^{i(A\theta'+B\phi')}\left[\frac{-\sin\theta'\,(\sin\phi' - i\,B\cos\phi') + i\,A\cos\theta'}{\sin\phi'}\right] \text{ for } m = 2, \quad (39)$$

$$\mathbb{U}^*_{gh,m} = \frac{1}{4\pi\bar{r}^2}\sum_{A=-a}^{a}\sum_{B=-a}^{a}\lambda^{(A,B)}_{gh}e^{i(A\bar{\theta}+B\phi')}[-(\cos\phi' + i\,B\sin\phi')] \text{ for } m = 3. \quad (40)$$

Consequentially, the kernel $\mathbb{T}^*_{ij}$ is computed by

$$\mathbb{T}^*_{ij} = (\sigma^*_{ik}\hat{n}_k)_j = \frac{C_{ikAB}n'_k\left(\mathbb{U}^*_{Aj,B} + \mathbb{U}^*_{Bj,A}\right)}{2} \quad (41)$$

Our task now is to treat the following domain integral in Eq. (14) [3]

$$D_j = -\int_R \vartheta_{ik}T_{,k}\mathbb{U}^*_{ij}dR \quad (42)$$

The domain integral must be redefined in the transferred domain as

$$D_j = -\int_{R'}\Gamma_{i'k'}T_{k'}\mathbb{U}^*_{i'j'}dR' \quad (43)$$

where

$$\Gamma_{i'k'} = C_{ijkl}\,\mathbb{K}_{11}\sqrt{\frac{\Omega}{\forall^3}}\begin{pmatrix}\alpha'_{11} & \alpha'_{12} & \alpha'_{13}\\ \alpha'_{21} & \alpha'_{22} & \alpha'_{23}\\ \alpha'_{31} & \alpha'_{32} & \alpha'_{33}\end{pmatrix}\begin{pmatrix}\sqrt{\forall}/\mathbb{K}_{11} & -\mathbb{K}_{12}/\mathbb{K}_{11} & B_1\\ 0 & 1 & B_2\\ 0 & 0 & B_3\end{pmatrix} \quad (44)$$

Now, the domain integral can be transformed to the boundary S' as

$$D_j = \int_{S'}\Gamma_{i'k'}\left[\left(T\mathbb{W}^*_{i'j'k',n'} - \mathbb{W}^*_{i'j'k',n'}T_{,n'}\right)\mathbb{b}'_{n'} - TU^*_{i'j'}\mathbb{b}_{k'}\right]dS' \quad (45)$$

where $\mathbb{W}^*_{i'j'k'}$ is a new kernel function, satisfying

$$W^*_{i'j'k',n'n'} = U^*_{i'j',k'} \quad (46)$$

in which

$$U^*_{g'h'} = \frac{G'(\theta,\phi)}{4\pi r} \quad (47)$$

where

$$G'^{(\theta,\phi)} = \sum_{A=-a}^{a}\sum_{B=-a}^{a}\lambda'^{(A,B)}_{g'h'}e^{i(A\theta+B\phi)},\ (g,h = 1,2,3) \quad (48)$$

Similarly, the coefficients $\hat{\lambda}^{(A,B)}_{g'h'}$ are determined by [3]

$$\lambda'^{(A,B)}_{g'h'} = \frac{1}{4\pi^2}\int_{-\pi}^{\pi}\int_{-\pi}^{\pi}H'_{g'h'}(\theta,\phi)e^{-i(A\theta+B\phi)}d\theta d\phi \quad (49)$$

After determining the coefficients $\lambda'^{(\mathbb{a},\mathbb{b})}_{g'h'}$ using Eq. (49), our next goal is to determine $W^*_{i'j'k'}$. $U^*_{g'h'}$ can be computed by

$$U^*_{g'h'} = \frac{1}{4\pi r'}\sum_{A=-a}^{a}\sum_{B=-a}^{a}\lambda'^{(A,B)}_{g'h'}e^{i(A\theta+B\phi)},\ (g,h = 1,2,3) \quad (50)$$

Now, Eq. (46) in the spherical coordinates can be expressed as

$$\frac{\partial^2\mathbb{W}^*_{i'j'k'}(\theta,\phi)}{\partial\hat{\phi}^2} + \cot\phi\frac{\partial\mathbb{W}^*_{i'j'k'}(\theta,\phi)}{\partial\phi} + \frac{1}{\sin^2\phi}\frac{\partial^2\mathbb{W}^*_{i'j'k'}(\theta,\phi)}{\partial\theta^2} = \kappa_{i'j'k'}(\theta,\phi) \quad (51)$$

where

$$\mathbb{W}^*_{i'j'k'}(\theta,\phi) = \sum_{A=-a}^{a}\sum_{B=-a}^{a}S'^{(\mathbb{a},\mathbb{b})}_{i'j'k'}e^{i(\mathbb{a}\theta+\mathbb{b}\phi)} \quad (52)$$

Also, $K_{i'j'k'}(\theta,\phi)$ and $U^*_{g'h',m'}$ are given in [3]

By using (52), the unknown coefficients $S'^{(\mathbb{a},\mathbb{b})}_{i'j'k'}$ can be calculated using the same manner as [3]. Then $\mathbb{W}^*_{i'j'k',n'}$, can be derived as follows

$$\mathbb{W}^*_{i'j'k',n'} = \frac{1}{r}\sum_{A=-a}^{a}\sum_{B=-a}^{a}S'^{(A,B)}_{i'j'k'}e^{i(A\theta+B\phi)}(i\,B\cos\theta\cos\phi - i\,A\,\sin\theta\,/\sin\phi) \text{ for } n = 1 \quad (53)$$

$$\mathbb{W}^*_{i'j'k',n'} = \frac{1}{r}\sum_{A=-a}^{a}\sum_{B=-a}^{a}S'^{(A,B)}_{i'j'k'}e^{i(A\theta+B\phi)}\left(i\,B\,\sin\theta\cos\phi + i\frac{A\cos\theta}{\sin\phi}\right) \text{ for } n = 2 \quad (54)$$

$$\mathbb{W}^*_{i'j'k',n'} = \frac{1}{r}\sum_{A=-a}^{a}\sum_{B=-a}^{a}S'^{(A,B)}_{i'j'k'}e^{i(A\theta+B\phi)}(-i\,B\,\sin\phi) \text{ for } n = 3 \quad (55)$$

4 Numerical Results and Discussion

BEM has been built using quadratic isoparametric elements, where the 8-point Gauss quadrature rule was used with double precision for the numerical integrations. Alumina (Al_2O_3) was considered in the calculations with the elastic stiffness coefficients as given in [29]

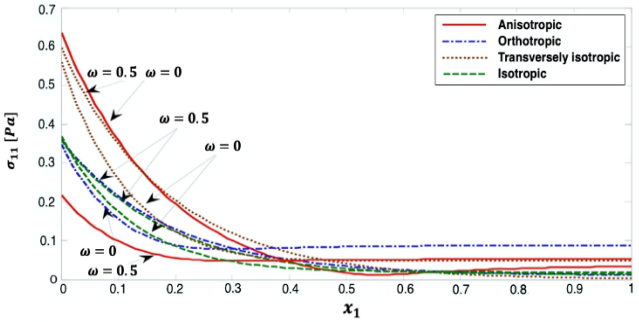

Fig. 1: Distribution of thermal stress $\boldsymbol{\sigma_{11}}$ for different materials with impact of rotation.

Figure 1 shows how the thermal stress σ_{11} changes for anisotropic, orthotropic, transversely isotropic, and isotropic materials with x_1-axis in the absence $(\omega = 0)$ and presence $(\omega = 0.5)$ of rotation. The distribution of thermal stress σ_{11} for four materials in the identical scenario along the x_1-axis. The curves for orthotropic, transversely isotropic, and isotropic materials show that the distribution of thermal stress σ_{11} grows with rotation, while it decreases with rotation for anisotropic materials.

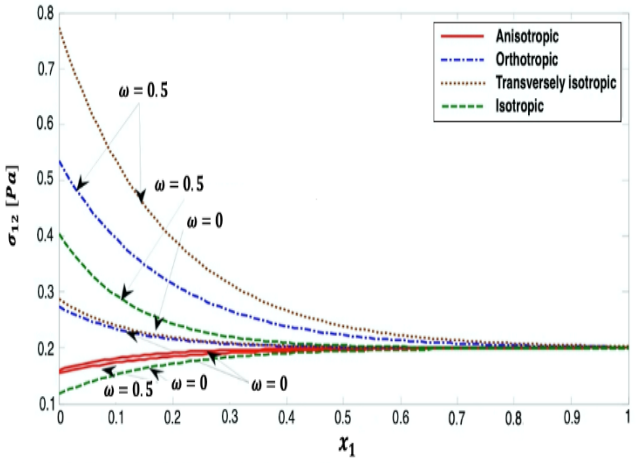

Fig. 2: Distribution of thermal stress $\boldsymbol{\sigma_{12}}$ for different materials with impact of rotation.

Figure 2 shows how the thermal stress σ_{12} changes for anisotropic, orthotropic, transversely isotropic, and isotropic materials with x_1-axis in the absence $(\omega = 0)$ and presence $(\omega = 0.5)$ of rotation. The distribution of thermal stress σ_{12} for four materials in the identical scenario along the x_1-axis except for anisotropic materials and non-rotating isotropic materials. The curves for orthotropic, transversely isotropic, and isotropic materials show that the distribution of thermal stress σ_{12} grows with rotation, while it decreases with rotation for anisotropic materials.

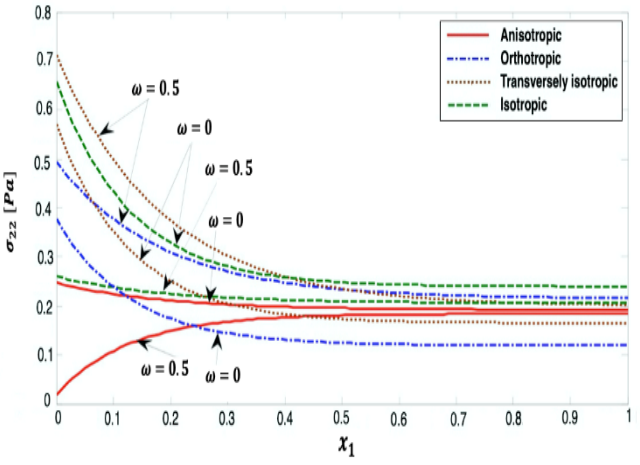

Fig. 3: Distribution of thermal stress $\boldsymbol{\sigma_{22}}$ for different materials with impact of rotation.

Figure 3 shows how the thermal stress σ_{22} changes for anisotropic, orthotropic, transversely isotropic, and isotropic materials with x_1-axis in the absence $(\omega = 0)$ and presence $(\omega = 0.5)$ of rotation. The distribution of thermal stress σ_{22} for four materials in the identical scenario along the x_1-axis except for anisotropic materials. The curves for orthotropic, transversely isotropic, and isotropic materials show that the distribution of thermal stress σ_{22} grows with rotation, while it decreases with rotation for anisotropic materials.

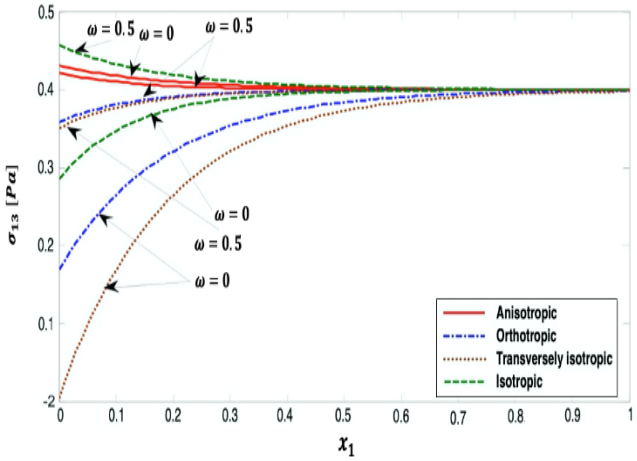

Fig. 4: Distribution of thermal stress $\boldsymbol{\sigma_{13}}$ for different materials with impact of rotation.

Figure 4 shows how the thermal stress σ_{13} changes for anisotropic, orthotropic, transversely isotropic, and isotropic materials with x_1-axis in the absence $(\omega = 0)$ and presence $(\omega = 0.5)$ of rotation. The distribution of thermal stress σ_{13} for four materials in the identical scenario along the x_1-axis except for anisotropic and rotating isotropic materials. The curves for orthotropic, transversely isotropic, and isotropic materials show that the distribution of thermal stress σ_{13} grows with rotation, while it decreases with rotation for anisotropic materials.

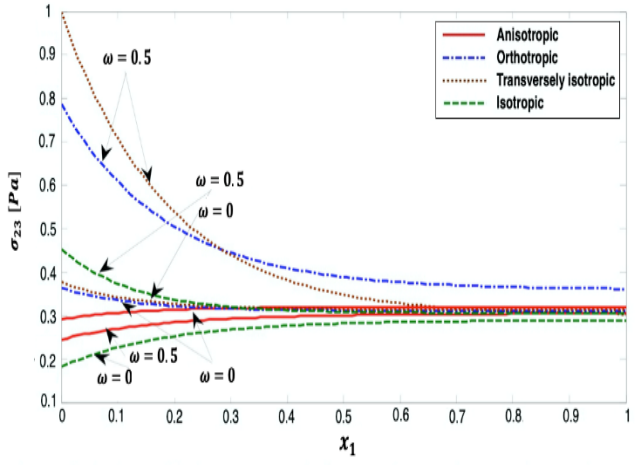

Fig. 5: Distribution of thermal stress $\boldsymbol{\sigma_{23}}$ for different materials with impact of rotation.

Figure 5 shows how the thermal stress σ_{23} changes for anisotropic, orthotropic, transversely isotropic, and isotropic materials with x_1-axis in the absence $(\omega = 0)$ and presence $(\omega = 0.5)$ of rotation. The distribution of thermal stress σ_{23} for four materials in the identical scenario along the x_1-axis except for anisotropic and non-rotating isotropic materials. The curves for orthotropic, transversely isotropic, and isotropic materials show that the distribution of thermal stress σ_{23} grows with rotation, while it decreases with rotation for anisotropic materials.

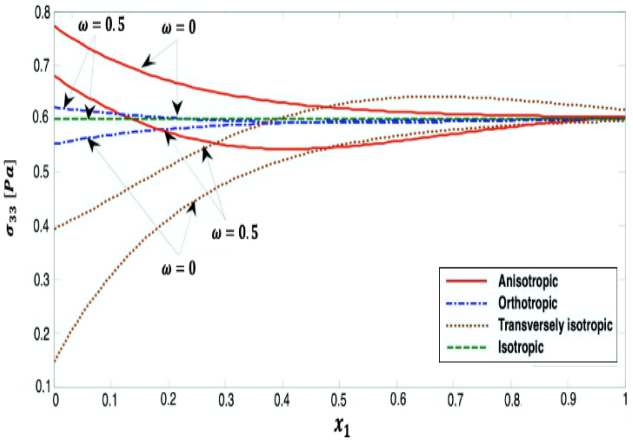

Fig. 6: Distribution of thermal stress $\boldsymbol{\sigma_{23}}$ for different materials with impact of rotation.

Figure 6 shows how the thermal stress σ_{33} changes for anisotropic, orthotropic, transversely isotropic, and isotropic materials with x_1-axis in the absence $(\omega = 0)$ and presence $(\omega = 0.5)$ of rotation. The distribution of thermal stress σ_{33} for four materials in the identical scenario along the x_1-axis except for transversely isotropic and non-rotating orthotropic materials. Rotation has no influence on thermal stress σ_{33} in isotropic materials. The curves for orthotropic and transversely isotropic materials show that the distribution of thermal stress σ_{33} grows with rotation, while it decreases with rotation for anisotropic materials.

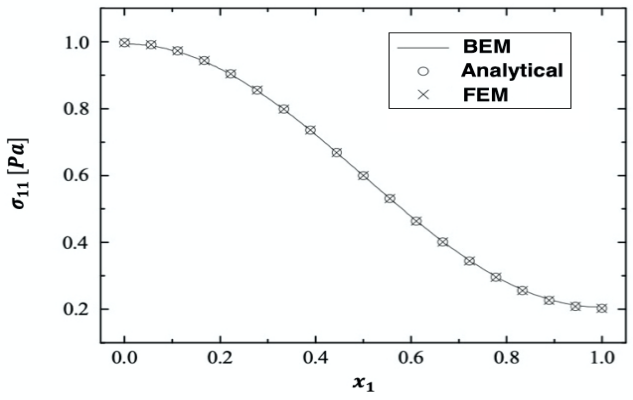

Fig. 7: Thermal stress $\boldsymbol{\sigma_{11}}$ distribution along $\mathbf{x_1}$**-axis** for Analytical, FEM, and BEM methods.

Figure 7 compares a special case of the present BEM thermal stress σ_{11} distribution along the x_1-axis to the analytical results of Ramady et al. [30] and the finite element method (FEM) results of Ferguson and Mikkelsen [31]. The present BEM, Analytical, and FEM all agree extremely well. Thus, the proposed method's validity was proven.

5 Conclusions

The boundary element approach was utilized in this study to investigate the effect of rotation on thermal stresses in anisotropic materials. As is well known in the BEM formulation, the heat effect introduces an additional volume integral, forcing domain discretization, causing the boundary element technique to lose its advantages. The present 3D BEM employs the exact transformation technique, which entails analytically translating the extra domain integral to the border while performing no internal treatments. To account for thermoelastic effects in anisotropic materials, BEM analysis was used to re-express the fundamental solutions and their derivatives as double-Fourier series. This analytical transformation approach has fully restored the BEM's distinctive requirement that just the boundary be discretized. Furthermore, the evaluations revealed that the 3D BEM approach is not only efficient for modeling, but also effective in producing accurate solutions for thermal stress problems in anisotropic materials.

Funding: The authors did not receive support from any organization for the submitted work.

Data Availability Statement: All data generated or analysed during this study are included in this published article.

Conflicts of Interest: The authors declare no conflict of interest.

References

[1] Rao, K.S., Bapu, Rao M.N., Ariman, T., 1971. Thermal stresses in plates with circular holes. Nucl. Eng. Des. 15 (1), 97–112.

[2] Rizzo, F.J., Shippy, D.J., 1977. An advanced boundary integral equation method for three-dimensional thermoelasticity. Int. J. Numerical Methods Engng. 11, 1753–1768.

[3] Shiah, Y.C, Tan, C.L., 2014. The boundary integral equation for 3D general anisotropic thermoelasticity. CMES Comp. Model. Eng. Sci. 102 (6), 425–447.

[4] Fahmy MA. Boundary element algorithm for nonlinear modeling and simulation of three temperature anisotropic generalized micropolar piezothermoelasticity with memory-dependent derivative. International Journal of Applied Mechanics 2020, 12, 2050027. https://doi.org/10.1142/S1758825120500271

[5] Pasternak, I. , 2012. Boundary integral equations and the boundary element method for fracture mechanics analysis in 2D anisotropic thermoelasticity. Eng. Anal. Bound. Elem. 36 (12), 1931–1941.

[6] Pasternak, I. , Pasternak, R. , Pasternak, V. , Sulym, H. , 2017. Boundary element analysis of 3D cracks in anisotropic thermomagnetoelectroelastic solids. Eng. Anal. Bound. Elem. 7, 70–78.

[7] Pasternak, I. , Pasternak, R. , Sulym, H. , 2013. A comprehensive study on the 2D boundary element method for anisotropic thermoelectroelastic solids with cracks and thin inhomogeneities. Eng. Anal. Bound. Elem. 37 (2), 419–433 .

[8] Pasternak, I. , Pasternak, R. , Sulym, H. , 2016. A comprehensive study on Green's functions and boundary integral equations for 3D anisotropic thermomagnetoelectroelasticity. Eng. Anal. Bound. Elem. 64, 222–229.

[9] Shiah Y. C., Tuan N. A., and Hematiyan M. R. Direct transformation of the volume integral in the boundary integral equation for treating three-dimensional steady-state anisotropic thermoelasticity involving volume heat source. International Journal of Solids and Structures 2018 vol. 143, pp. 287-297. https://doi.org/10.1016/j.ijsolstr.2018.03.019

[10] Fahmy, M. A. and Toujani, M. Fractional Boundary Element Solution for Nonlinear Nonlocal Thermoelastic Problems of Anisotropic Fibrous Polymer Nanomaterials. Computation 2024, 12(6), 117. Doi: https://doi.org/10.3390/computation12060117

[11] Shiah, Y.C., Hsu, C.-L., Hwu, C. , 2014. Direct volume-to-surface integral transformation for 2D BEM analysis of anisotropic thermoelasticity. CMES-Comput. Model. Eng. Sci. 102 (4), 257–270.

[12] Wang, C.Y., Denda, M., 2007. 3D BEM for general anisotropic elasticity. Int. J. Solids Struct. 44, 7073–7091.

[13] Shiah Y.C. Analysis of thermoelastic stress-concentration around oblate cavities in three-dimensional generally anisotropic bodies by the boundary element method. International Journal of Solids and Structures 81 (2016) 350–360. https://doi.org/10.1016/j.ijsolstr.2015.12.008

[14] Shiah, Y.C., Chong, J.-Y., 2016. Boundary element analysis of interior thermoelastic stresses in three-dimensional generally anisotropic bodies. J. Mech. 32 (6), 725–735.

[15] Abouelregal AE, Ahmed IE, Nasr ME, Khalil KM, Zakria A, Mohammed FA. Thermoelastic processes by a continuous heat source line in an infinite solid via Moore–Gibson–Thompson thermoelasticity. Materials 2020, 13 (19), 4463. https://doi.org/10.3390/ma13194463

[16] Abouelregal AE, Yao SW, Ahmad H. Analysis of a functionally graded thermopiezoelectric finite rod excited by a moving heat source. Results in Physics 2020, 19, 103389. https://doi.org/10.1016/j.rinp.2020.103389

[17] Gao, X. W., 2003. Boundary element analysis in thermoelasticity with and without internal cells. Int. J. Numer. Methods Eng. 57 (7), 975–990.

[18] Fahmy, M. A. BEM Modeling for Stress Sensitivity of Nonlocal Thermo-Elasto-Plastic Damage Problems. Computation 2024, 12(5), 87. Doi: https://doi.org/10.3390/computation12050087

[19] Fahmy, M. A. and Alzubaidi, M. H. M. A boundary element analysis of quasi-potential inviscid incompressible flow in multiply connected airfoil wing. Journal of Umm Al-Qura University for Engineering and Architecture 2024. Doi: https://doi.org/10.1007/s43995-024-00063-3

[20] Fahmy, M. A. A time-stepping DRBEM for nonlinear fractional sub-diffusion bio-heat ultrasonic wave propagation problems during electromagnetic radiation. Journal of Umm Al-Qura University for Applied Sciences 2024. https://doi.org/10.1007/s43994-024-00178-2

[21] Camp, C. V., Gipson, G. S., 1992. Boundary Element Analysis of Nonhomogeneous Bi- harmonic Phenomena. Springer-Verlag, Berlin.

[22] Hematiyan, M. R., 2007. A general method for evaluation of 2D and 3D domain integrals without domain discretization and its application in BEM. Comput. Mech. 39 (4), 509–520.

[23] Fahmy, M. A., Alsulami, M. O. and Abouelregal, A. E. Three-Temperature Boundary Element Modeling of Ultrasound Wave Propagation in Anisotropic Viscoelastic Porous Media. Axioms 2023, 12, 473. https://doi.org/10.3390/axioms12050473

[24] Fahmy, M. A. Fractional Temperature-Dependent BEM for Laser Ultrasonic Thermoelastic Propagation Problems of Smart Nanomaterials. Fractal and Fractional 2023, 7(7), 536. https://doi.org/10.3390/fractalfract7070536

[25] Ting, T.C.T., Lee, V.G., 1997. The three-dimensional elastostic Green's function for general anisotropic linear elastic solid. Q. J. Mech. Appl. Math. 50, 407–426.

[26] Phan, A-V., Gray, L.J., Kaplan, T., 2005. Residue approach for evaluating the 3D anisotropic elastic Green's function: multiple roots. Eng. Anal. Bound. Elem. 29, 570–576.

[27] Buroni, F.C., Sáez, A. Unique and explicit formulas for Green's function in three-dimensional anisotropic

linear elasticity. J. Appl. Mech. 2013, 80, 051018–051011.

[28] Shiah, Y.C. Analytical transformation of the volume integral for the BEM treating 3d anisotropic elastostatics involving body-force. Comput. Methods Appl. Mech. Eng. 2014, 278, 404–422.

[29] Huntington, H.B., 1958. The Elastic Constants of Crystals. Academic Press, New York.

[30] Ramady, A., Dakhel, B., Balubaid, Mohammed, Mahmoud, S.R.. A mathematical approach for the effect of the rotation on thermal stresses in the piezo-electric homogeneous material. Computers and Concrete 2020, 25, 471-478

[31] Ferguson, O.V.; Mikkelsen, L.P. Three-Dimensional Finite Element Modeling of Anisotropic Materials using X-ray Computed Micro-Tomography Data. Software Impacts 2023, 17, 100523.